Aerosol and Air Quality Research, 16: 3012–3025, 2016

ISSN: 1680-8584 print / 2071-1409 online
doi: 10.4209/aaqr.2015.12.0683

Experimental Parametric Study of Frequency and Sound Pressure Level on the Acoustic Coagulation and Precipitation of $PM_{2.5}$ Aerosols

Mohsen Amiri[1,2], Asghar Sadighzadeh[1*], Cavus Falamaki[2]**

[1] *Safety & Environmental Lab, Nuclear Science and Technology Research Institute, AEOI, Tehran, Iran*
[2] *Chemical Engineering Department, Amirkabir University of Technology, Tehran, Iran*

ABSTRACT

The efficiency of particle removal for $PM_{2.5}$ aerosols using conventional separation systems is generally low. In this paper, acoustic precipitation and coagulation of aerosols as a preconditioning system is investigated experimentally. The results of experimental study concerning the effect of frequency and sound pressure level (SPL) on the acoustic coagulation and precipitation of $PM_{2.5}$ aerosols are presented. An acoustic particle conditioning setup was used to perform experiments at the resonance frequencies of 204, 550, 650 and 749 (Hz), and SPLs 140, 150, 155, 162 dB. All experiments were performed under ambient condition and similar initial concentration. The experimental results showed that the effect of acoustics on filtration efficiency is amplified by increasing the frequency and intensity. Eventually, at the frequency of 749 (Hz) and 162 (dB) the acoustic coagulation and precipitation efficiency reaches about 83% which is significant. The results of this study (experimentally and theoretically) prove the existence of a threshold in SPL (≥ 155 dB) at which the acoustic precipitation and coagulation efficiency increase rapidly, implying the importance of turbulence coagulation interactions at high intensity acoustic waves. In addition, a new empirical correlation was developed for the acoustic coagulation and precipitation efficiency with reasonable accuracy.

Keywords: Aerosol coagulation; Precipitation; Acoustic wave; Coagulation kernels; Turbulence interactions.

INTRODUCTION

One of the most difficult environmental challenges is the elimination of sub-micron aerosols from industrial flue gases. In fact, these particles constitute a major health hazard because of their ability to penetrate deeply into the respiratory system (Gallego-Juárez *et al.*, 1999). Conventional separation technologies for collecting aerosols include electrostatic precipitators, cyclones and filter bags. However, the removal efficiency of these devices reduces severely for $PM_{2.5}$ particles (Vincent, 1995). In order to improve the removal efficiency of fine particle, aerosol-preconditioning systems are required to form larger particles before entering separation devices.

Acoustic agglomeration is a process, which increases the average particle size of aerosols. In fact, by applying acoustic waves to a fluid, which contains fine particles, different forces are exerted on them. These forces accelerate the particles' motion. Finally, particles will collide and coagulation will happen. Afterwards, remarkable percentage of agglomerated particles precipitate and the rest could be removed by other conventional separation systems.

The study of acoustic agglomeration started between 1926–1927 when Wood used high power ultrasonic waves to observe the physical effects of waves in liquids (Wood and Loomis, 1927). Patterson and Cawood performed a similar experiment in gaseous medium and for the first time observed acoustic agglomeration in standing waves in 1931 (Patterson and Cawood, 1931). In Germany, independent investigations were conducted by Brandt and Hiedemann (Brandt and Hiedemann, 1936). They checked different frequencies and found that acoustic coagulation in the hearing range frequencies is better carried out than that in the ultrasonic ones.

In the following section, some examples of laboratory investigations conducted in this field are provided. Gallego-Juárez *et al.* (1999) studied the application of acoustic agglomeration in order to reduce fine particle emission from coal plant exhaust in a pilot plant scale. Results indicated that by using acoustic filters, the number concentration of particles decreased to about 40%. Martin and Ezekoye, (1997) investigated the removal of soot particles from a static chamber by an intense acoustic field. The results showed

* Corresponding author.
Tel.: 98 21 88221093; Fax: 98 21 88221095
E-mail address: asadigzadeh@aeoi.org.ir
** Corresponding author.
Tel.: 98 21 64543160; Fax: 98 21 66405847
E-mail address: c.falamaki@aut.ac.ir

that acoustic filtration increases the rate of soot removal by a factor of two over acoustically induced sedimentation alone. They also stated that agglomerated soot particles, which are acoustically levitated in the chamber, provide stable anchor points throughout the flow which capture fine soot particles. The acoustic agglomeration rate of TiO_2 particles as well as the glycol mist at 21 kHz and 160 dB was investigated by Somers *et al.* (1991). Ammonium chloride particles were acoustically agglomerated experimentally by Cheng in the frequency range 600 to 3000 Hz and sound pressure level of 145 dB to 155 (Cheng *et al.*, 1983). Moreover, there are some other experimental and theoretical investigations (Tavossi, 1986; Temkin, 1994; Liu *et al.*, 2009; Wang *et al.*, 2011; Guo *et al.*, 2012).

The main purpose of this paper is to present and discuss the results of an experimental study covering the effects of frequency and SPL on the acoustic coagulation of $PM_{2.5}$ particles.

Theoretical Study

There are many acoustic agglomeration mechanisms. The most conventional ones, as discussed in many papers, are orthokinetic interactions and hydrodynamic interactions. However, the presence of turbulent interaction in this process, which requires high Sound Pressure Levels (SPL), will highly increase acoustic agglomeration and precipitation efficiency. High-intensity acoustic fields applied to an aerosol may induce interaction effects among the suspended particles, giving rise to collisions and agglomerations.

General Dynamic Equation

The first treatment of the effect of particle coagulation on the discrete particle size distribution is presented by Smoluchowski (Smoluchowski, 1916). Under the assumption that all particles are spherical, he showed that the dynamic equation for the discrete size spectrum N_k (t) is expressed as Eq. (1)

$$\frac{dN_k}{dt} = \frac{1}{2}\sum_{i+j=k} K(\upsilon_i,\upsilon_j)N_iN_j - N_k\sum_{i=1}^{\infty} K(\upsilon_i,\upsilon_k)N_i \,, \tag{1}$$

where $K(\upsilon_i, \upsilon_j)$ expressed in dimensions of volume per unit time, is the collision frequency function (kernel) between particle of volume υ_i and υ_j. The first term on the right-hand side (RHS) of Eq. (1) is the rate (per unit volume) at which k-particles are created from the collision of (j = k – i)-particles with i-particle sizes. The second term is the rate at which k-particles are eliminated by collisions with other ones (Crowe, 2005). In the following section, the main acoustic coagulation kernels (Brownian, orthokinetic, hydrodynamic and turbulence) are discussed.

Brownian Coagulation

Brownian coagulation was found to play a substantial role particularly for sub-micron particles. The initial mean diameter of particles in the simulated cases is less than one micron which means a large fraction of particles is in submicron range. Thus, the contribution of Brownian coagulation is comprised (Sheng and Shen, 2006). The kernel for Brownian coagulation near the continuum regime, with Cunningham slip correction (C) applied, is as Eq. (2)

$$K^B = \frac{2kT}{3\mu}(d_1 + d_2)\left(\frac{C_1}{d_1} + \frac{C_2}{d_2}\right) \tag{2}$$

where K^B is Brownian coagulation frequency kernel ($m^3\ s^{-1}$), k is Boltzmann constant ($J\ K^{-1}$), T is absolute temperature (K), μ is dynamic viscosity of air ($kg\ m^{-1}\ s^{-1}$), C is Cunningham correction factor and d is particle diameter (m), subscription 1 and 2 are related to particle one and two, respectively.

Orthokinetic Interaction

One of the first theories presented to explain the phenomenon of acoustic agglomeration, was the orthokinetic interactions. This hypothesis was presented by Mednikov in 1965 and some years later it was proved by other researchers (Mednikov, 1965). According to this model, particles of various sizes in the presence of acoustic waves have various velocities in a way that smaller particles oscillate approximately of the same speed as the velocity of acoustical field and the larger particles have less velocity and are almost stationary. As a result, particles with different sizes move relative to each other (Dong *et al.*, 2006).

In one acoustic cycle, each large particle will sweep a specific volume by its motion in respect to smaller particles. This volume is the known as agglomeration volume (Mednikov, 1965). If any fine particles are present in the agglomeration volume, they will collide with and thus, will be gathered by the large particles. Afterwards, the volume may be refilled by particles coming from outside, driven by the other interactions like scattering, hydrodynamic or Brownian interactions. (Sheng and Shen, 2006).

Orthokinetic interaction has a relatively high dependence on frequency and particle size. Acoustic agglomeration of ash particles in traveling waves was investigated by Liu *et al.* (2009). Their results showed that the particle removal rate decreased with increasing acoustic intensity and was crucially frequency-dependent. They explained that orthokinetic theory was the governing mechanism of this process. The orthokinetic coagulation kernel function is expressed as Eq. (3) (Mednikov, 1965).

$$K^{Ort}_{Mednikov} = \frac{1}{2}(d_1 + d_2)^2\,\eta_{12}U_g \tag{3}$$

where K^{Ort} is Mednikov orthokinetic coagulation frequency kernel ($m^3\ s^{-1}$), U_g is the velocity amplitude of sound wave ($m\ s^{-1}$) and η_{12}, is the relative entrainment factor between particles 1 and 2, is defined as Eq. (4) (Mednikov, 1965).

$$\eta_{12} = \sqrt{\eta_1^2 + \eta_2^2 - 2\eta_1\eta_2\cos(\phi_1 - \phi_2)} \tag{4}$$

where η_1, η_2 are the entrainment factors (the entrainment factor is described as the ratio of the velocity amplitudes of

the particle oscillations and the gas) of the particles 1 and 2, and ϕ_1, ϕ_2 are the phase differences between the acoustic wave and the particle vibrations, respectively. These parameters can be evaluated by the complex entrainment equation following Temkin (1981) (Sheng and Shen, 2006) Eq. (5).

$$H = \frac{1+\frac{3}{2}\sqrt{\omega\tau_p\delta} - i\frac{3}{2}\left(\omega\tau_p\delta + \sqrt{\omega\tau_p\delta}\right)}{1+\frac{3}{2}\sqrt{\omega\tau_p\delta} - i[(1+\frac{\delta}{2})\omega\tau_p + \frac{3}{2}\sqrt{\omega\tau_p\delta}]} \quad (5)$$

where H is complex entrainment function, ω is angular frequency of acoustic wave, τ_p is particle relaxation time (s) and δ is ratio of air density and particle density. The magnitude and phase of *H* are the entrainment factor and phase delay of a particle, respectively given by Eq. (6).

$$\begin{cases} \eta = |H| \\ \phi = \tan^{-1}\left(\frac{\mathrm{Im}(H)}{\mathrm{Re}(H)}\right), \end{cases} \quad (6)$$

where η is entrainment factor of a particle in a sound wave, Im and Re stand for the imaginary and real parts, respectively.

Nonetheless, both assumptions in the Mednikov model Eq. (2) are theoretically controversial because the effects of the interactions between two particles and also between particles and the acoustic waves on the coagulation were ignored (Sheng and Shen, 2006). Considering the scattering interactions between the two particles, Song (1990) derived a modified relative entrainment factor as Eq. (7).

$$\eta_{s12} = |H_1 - H_2 + G_{12}| \quad (7)$$

where η_{s12} is modified relative entrainment factor between two particles 1 and 2 and G_{12} is the scattering interaction function determined on the surface of the collision particles (Song *et al*., 1994). With this factor, the Song's orthokinetic coagulation kernel function is expressed as Eq. (8) (Song, 1990):

$$K_{Song}^{Ort} = \frac{1}{2}(d_1 + d_2)^2 U_g \eta_{s12} \quad (8)$$

where K^{ort} is the Song orthokinetic coagulation frequency kernel ($m^3\ s^{-1}$).

Hydrodynamic Interactions

Based on the orthokinetic interaction, the particles with the same dimensions do not collide with each other because the relative velocity between the particles is zero. However, coagulation of particles with identical dimensions (monodisperse particles) under the influence of acoustic waves has been observed experimentally (Shaw and Tu, 1979). This fact eventually led to the theory of hydrodynamic interaction (Song, 1990).

The hydrodynamic interaction occurs when the line joining the centers of two particles is perpendicular to the direction of acoustic velocity. In this situation, two interacting particles form an effective jet and the gas velocity relative to the particles would be stronger between the particles than that in the outside. From Bernoulli's hydrodynamic principle, this velocity difference results in a net pressure force which drag two particle toward each other. Consequently, it increases the possibility of collisions and coagulations among particles (Song, 1990).

In an ideal fluid, the hydrodynamic coagulation kernel function can be described by the classic expression of König (1891) Eq. (9) (Ezekoye and Wibowo, 1999; Sheng and Shen, 2006).

$$K_{Konig}^{Hyd} = \frac{2\sqrt{3}\rho_g U_g^2}{36\mu}\frac{(d_1 d_2)^2}{d_1 + d_2} \quad (9)$$

where K^{hyd} is the König hydrodynamic coagulation kernel function ($m^3\ s^{-1}$).

Danilov indicates that the viscosity of a gas could increase the interaction force by several orders (Danilov and Mironov, 1984). However, Danilov's hydrodynamic forces are valid only for the interacting particles fixed in the space (i.e., not entrained) and located far away from each other so that the viscous portion of the scattered wave field can be neglected (Song *et al.*, 1994).

Song derived a modified theoretical model by arguing that both effects of entrainment and of rotational wave interactions (which Danilov neglected) should be included in the force expression. The Song's hydrodynamic coagulation kernel function in is given by Eq. (10) (Song *et al.*, 1994; Ezekoye and Wibowo, 1999).

$$K_{Song}^{Hyd} = \frac{\sqrt{3}\rho_g U_g^2}{144\pi\mu}\frac{(d_1 d_2)^2}{d_1 + d_2} g_{12} = \left(\frac{g_{12}}{4\pi^2}\right) K_{Konig}^{Hyd} \quad (10)$$

where K^{Hyd} is Song's hydrodynamic coagulation kernel function ($m^3\ s^{-1}$) and g_{12} is a complex hydrodynamic interaction function between particle 1 and 2, detailed in (Song, 1990).

Turbulence Induced Interaction

Despite the studies done previously on the later theories, there is not any reliable prediction based on them for high-intensity conditions. Mednikov suggested in his initial research on acoustic coagulation of particles that the acoustically generated turbulence played an important role in this process (Mednikov, 1965). Then, Chou *et al.* (1981) claimed that this turbulence was the predominant mechanism of coagulation for high sound pressure levels of 160 (dB) (Lee *et al.*, 1981). Therefore, they proposed that all acoustic coagulation tests should be performed at the sound pressure levels over 160 (dB).

Saffman and Turner (1956) and Levich (1962) have proposed theories on coagulation rate in a turbulent flow. The collision between particles in a turbulent flow are considered to be caused by two principally independent mechanisms,

turbulent-diffusional and turbulent-inertial interactions. Regarding turbulent-diffusion, particles may collide with each other because of their disparate velocities as a result of the spatial non-homogeneity of a turbulent flow. On the other hand, turbulent inertial collisions are caused by relative motion of the particles which cannot pursue rapid local turbulent motions of the fluid (Chou *et al.*, 1981).

In these interactions the coagulation processes, in effect, occur in the small eddies whose sizes are characterized by the Kolmogorov micro-scale Eq. (11) (Chou *et al.*, 1981).

$$\zeta = \left(\frac{\nu^3}{\varepsilon}\right)^{1/4} \tag{11}$$

where ζ is Kolmogorov micro-scale (m), ε is the time rate of energy dissipation of turbulence per unit mass (J kg^{-1} s^{-1}) and ν is the kinematic viscosity of the ambient gas-medium (m^2 s^{-1}). E.g., in the condition of 162 dB and 749 Hz, ζ is about 62 μm.

Diffusional Turbulent Interaction

In the case that the particle motion is fully entrained against eddy motions, the spatial inhomogeneity of turbulent velocity in the minuscule eddies establishes a particle motion thoroughly stochastic in nature (Chou *et al.*, 1981). Particles that are much smaller than the Kolmogorov micro-scale ζ and fully entrained by the turbulent eddy motions will move to the bulk of the fluid in a chaotic fashion. Besides the fact that it has a much faster rate, this type of particle movement is very similar to that of the Brownian motion (Lee *et al.*, 1981). The turbulent diffusional coagulation kernel function is determined as Eq. (12) (Saffman and Turner, 1956).

$$K^{TD} = \frac{1.3}{8}\left(d_1 + d_2\right)^3 \left(\frac{\varepsilon}{\nu}\right)^{1/2} \tag{12}$$

where K^{TD} is the turbulent diffusional coagulation kernel function (m^3 s^{-1}).

Inertial Turbulent Interaction

In such a way that the particles are not fully entrained by the turbulent eddy motions, they collide with each other according to their different velocities and relaxation times. Because of the close relationship between this process and the particle inertia, this coagulation mechanism is entitled as the turbulent inertial interaction (Lee *et al.*, 1981).

Saffman and Turner (1956) also contemplate turbulent coagulation with inertial effects. They used the particle equations of motion and statistical arguments for isotropic turbulent flow to achieve the turbulent inertial coagulation kernel function as Eq. (13).

$$K^{TI} = \frac{5.7}{4}\left(d_1 + d_2\right)^2 \left|\tau_{p,1} - \tau_{p,2}\right| \left(\frac{\varepsilon^3}{\nu}\right)^{\frac{1}{4}} \tag{13}$$

where K^{TI} is the turbulent diffusional coagulation kernel function (m^3 s^{-1}).

Certainly, the introduction of relative motion between particles will improve the opportunity of particle collisions and therefore, play an important role in coagulation process. Since the difference in density between particles and ambient medium are much larger in air that in liquid, this effect is much more important in air (Chou *et al.*, 1981).

Some other researchers have examined the effect of turbulence on acoustic particle coagulation (Lee *et al.*, 1981; Malherbe *et al.*, 1988). Malherbe suggested that acoustic coagulation in high intensity might be related to the sharp increase of turbulence within the system. In addition, Malherbe claimed that turbulence seems to appear between (152–153 dB) (Malherbe *et al.*, 1988). Also, A. Sadigzadeh showed experimentally the existence of a threshold at the sound pressure level of 150 dB since turbulence eddies began to form at the antinode region of acoustic wave (Sadighzadeh, 1990). Nonetheless, there are few experimental investigations in this field.

Total Acoustic Coagulation Kernel

The total acoustic coagulation kernel is a combination of all mechanisms included in the process, e.g., Brownian, orthokinetic, hydrodynamic and turbulence kernels. A simple addition of the coagulation kernel functions is described as Eq. (14)

$$K^{Tot} = K^{B} + K^{Ort} + K^{Hyd} + K^{TD} + K^{TI} \tag{14}$$

K^{Tot} is often used as the total coagulation kernel function (m^3 s^{-1}), (Ezekoye and Wibowo, 1999; Sheng and Shen, 2006).

Comparison of Different Interactions

Concerning the study of the importance of each acoustic coagulation interaction in the total acoustic coagulation kernel, a sensitivity analysis is performed with respect to some parameters, i.e., the frequency, particle size and sound pressure level.

Improvement of Song's Models

As mentioned in section *Orthokinetic Interaction and Hydrodynamic Interaction, So*ng made some improvements in the orthokinetic and hydrodynamic models (Song *et al.*, 1994). The ratio of K^{Ort} of Song's orthokinetic model to Mednikov model is indicated by α and the ratio of K^{Hyd} of Song's hydrodynamic model to König model is indicated by β as in Eq. (15).

$$\begin{cases} \alpha = \dfrac{K_{Song}^{Ort}}{K_{Mednikov}^{Ort}} = \dfrac{\eta_{s12}}{\eta_{12}} \\ \beta = \dfrac{K_{Song}^{Hyd}}{K_{Konig}^{Hyd}} = \left(\dfrac{g_{12}}{4\pi^2}\right) \end{cases} \tag{15}$$

The evolution of α and β parameters with respect to the particle diameter at the condition of 749 Hz and 162 dB (one of experiment conditions) is shown in Fig. 1.

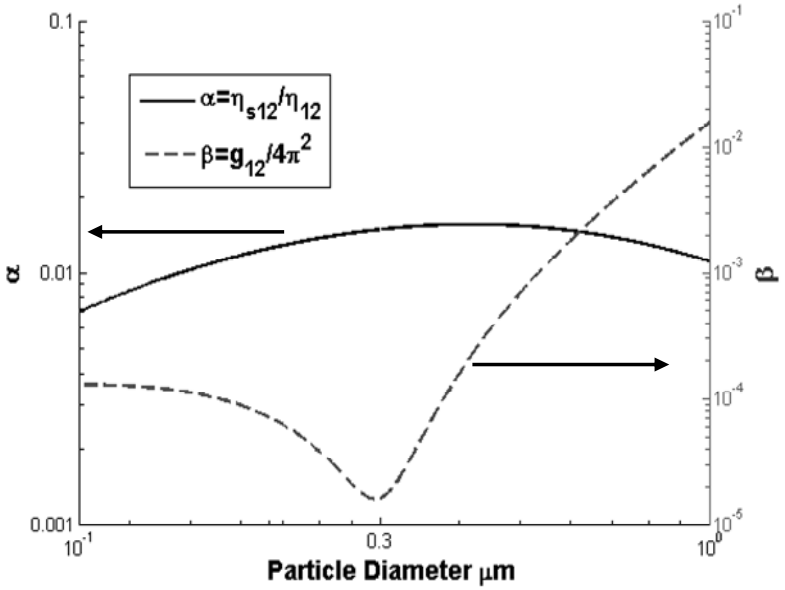

Fig. 1. The calculated collision efficiency (α) and hydrodynamic interaction factor (β). The data were calculated for the collision between a particle of 0.3 μm and a particle of 0.1–1 μm.

Actually α defines the collision efficiency under the orthokinetic mechanism. Its value is normally less than one, which means that, due to the scattering interactions, only some part of the small particles in the agglomeration volume can be swept and cleaned by the large particle in an acoustic cycle (Sheng and Shen, 2006). In addition, β describes a hydrodynamic factor which transforms the König hydrodynamic kernel to Song kernel. Theoretically, the König expression is based on the hydrodynamic interaction of particles in an ideal fluid i.e., neglects the viscosity-associated effects. Including the effects of both the viscous waves and the particle entrainment in acoustic waves, Song's approximation was expressed as a modified König equation with a factor of β. It can be seen that this factor is much less than one, particularly for the coagulation between particles with similar sizes (0.3 μm). Considering the fact that Song actually improved orthokinetic and hydrodynamic interaction kernels, in the following section, we chose to use Song's kernels with other three kernels in Eq. (14) and compare all of them together to find out which one is more important.

All Kernels

The evolution of acoustic coagulation kernels of a particle with the size 0.3 μm with particles in the range of (0.1–2 μm) at 162 dB and 749 Hz is illustrated in Fig. 2. For coagulation of a particle with (0.3 μm) diameter and a particle in the range of (0.1–1 μm), Brownian coagulation is the most important kernel and after that, turbulent diffusional and inertial have a considerable contribution in the total kernel. However, for the coagulation of a particle with (0.3 μm) diameter and a particle in the range of (0.1–1 μm), according to Eq. (2) Brownian kernel almost has no dependency to evolution of particle diameter, which is clear in Fig. 2. In addition, Turbulent inertial has a significant increase and becomes the most important kernel, which is because of the improvement in term $(1/\tau_1–1/\tau_2)$ with respect to the particle (2) diameter in Eq. (13). Besides, hydrodynamic kernel shows that it could be comparable with other kernels when the second particle becomes larger which is due to the significant increase in hydrodynamic factor (described in section *Improvement of Song's Models*). Turbulent diffusional kernel shows a slow variation with particle (2) diameter. Orthokinetic kernel shows the minimum value in all particle diameter in comparison with other kernels.

Another question is which interactions is dominant and which one is more dependent on sound pressure level in high intensity acoustic waves (≥ 155 dB). The importance of this question arises from the fact that the difference of acoustic coagulation with other coagulation conditions is in the presence of acoustic waves with specified intensity and frequency in the system. Accordingly, the evolution of acoustic coagulation kernels (particle-1 (0.3 μm) and particle-2 (0.8 μm)) with respect to the sound pressure level (140–162 dB) at 749 Hz is shown in Fig. 3(a). Brownian coagulation kernel has the most contribution in the total kernel in the range of SPL (140–150). Because Brownian coagulation kernel has no dependency on acoustic wave parameter (Eq. (2)), no variation in K_B with respect to the SPL occurs. However, a significant improvement in K_{Tot} arises after SPL 155, for which the most important reason is the rapid improvements of turbulent kernels (K^{TI} and K^{TD}). The turbulent acoustic coagulation depends only on the energy dissipated in the system (Malherbe *et al.*, 1988). As a result, in high intensity acoustic waves turbulent dissipation rate (ε) improve so high, which cause fast increase of KTI and K^{TD} (Eqs. (12) and (13)). Faster increase of K^{TI} compared with K^{TD} is because of the power of ε parameter in corresponding equations (Eqs. (12) and (13)) which are $\varepsilon^{3/4}$ and $\varepsilon^{1/2}$ respectively. Briefly, it can be said that at high intensity acoustic field with rapid chaotic movement of small turbulent eddies, the possibility of collision between particles, which are carried by eddies, become so high and as

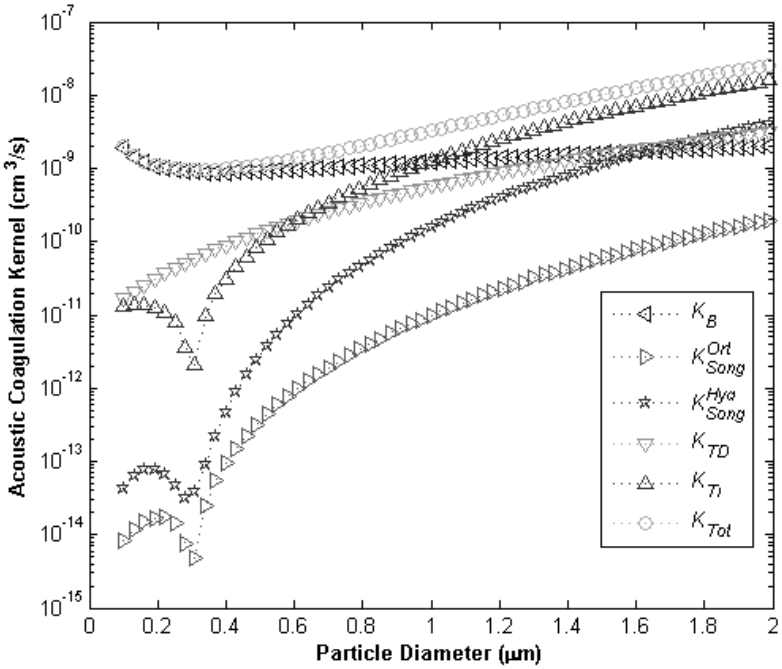

Fig. 2. Evolution of acoustic coagulation kernels (logarithmic scale) of a particle with (0.3 μm) with particles in the range of (0.1–2 μm) at 162 dB and 749 Hz (K_B-Brownian Kernel, K^{Ort}- Song Orthokinetic Kernel, K^{Hyd}-Song Hydrodynamic Kernel, K^{TD}-Turbulent Diffusional Kernel, K^{TI}-Turbulent Inertial Kernel and K^{Tot}-Total Kernel).

a result coagulation improves significantly. Malherbe observed the sharp increase of turbulent dissipation rate (ε) at SPL of about 153 dB experimentally which is in good agreement with result shown in Fig. 3(a) (Malherbe *et al.*, 1988).

Evolution of acoustic coagulation kernels (particle-1 (0.3 μm) and particle-2 (0.8 μm)) with respect to the frequency (204–749 Hz) at 162 dB is demonstrated in Fig. 3(b). Except the Brownian coagulation kernel, all kernels increase with respect to frequency. Nevertheless turbulent kernels (K^{TI} and K^{TD}) (specifically K^{TI}) show significant improvement over others. In addition hydrodynamic and orthokinetic kernels show minimum variation with respect to the frequency in comparison with turbulent kernels. K_{Tot} shows an almost linear relationship on frequency unlike SPL (Fig. 3).

In the following sections, an experimental study of particle coagulation is presented. It is worth mentioning that all calculated parameters and physical properties in previous sections are based on experimental study conditions (discuss in the followings).

METHODS

The acoustic agglomeration system shown in Fig. 4 consists of an atomizer aerosol generator (TOPAS-ATM 230) which produce liquid aerosols by spray technique in the size of about 0.3 μm, particle counters (Grimm - model 7.309), an acoustic agglomeration-precipitation chamber, a signal generator (ARMA AGA-101), a sound level meter (CASELLA-CEL-450 and 485) and a power amplifier (ECOCHANG XPA6010). The agglomeration-precipitation chamber is assembled by using a vertical tube with the diameter of 54 mm and the length of 1.53 m. A horn is used to connect loudspeaker to the top of the chamber. An amplifier strengthens the output signal from the signal generator before feeding the loudspeaker. Experiments were performed at the frequencies of 204, 550, 650, 749 Hz and at the sound pressure levels of 140, 150, 155, 162 dB. Therefore, in each experimental run, frequency is kept fixed and the value of sound pressure level (SPL) has been changed in the four states (16 runs in total).

The acoustic measurement point was located at the end of the chamber because the axial variation of SPL in the agglomeration chamber measured was less than 1 dB. Fig. 5 depicts the influence of electric power on SPLs with respect to the different sound frequencies. The results show the SPLs at the outlet of the horn range from 129–164 dB for input powers of .01–14 W. The diluter reduces the concentration of particles at the particle counter inlet in the scale of (1 to 10^3 per cm^3). The particle counter is installed at the outlet of the chamber to measure real time Particle Size Distributions (PSDs) in the range of 0.26 μm to 2 μm.

In order to investigate the effects parameters, experiments are performed as follows. Firstly, the test chamber evacuated from fine particles by clean air stream from the filter (HEPA). After that, while the outlet line open, fine particles of D.O.P (Dioctyl phthalate C_6H_4 $(COOCH_2CH$ (C_2H_5) $C_4H_9)_2)$ enter to the chamber by the aerosol generator at the rate of 2.5 L min^{-1}. After turning off the aerosol generator, all of the valves are closed and the acoustic waves are applied in the acoustic chamber in the specified time, intensity and frequency. Immediately afterward, the particle counter device starts to take online sample from the acoustic chamber bottom. As a result, it shows the online PSD in terms of time.

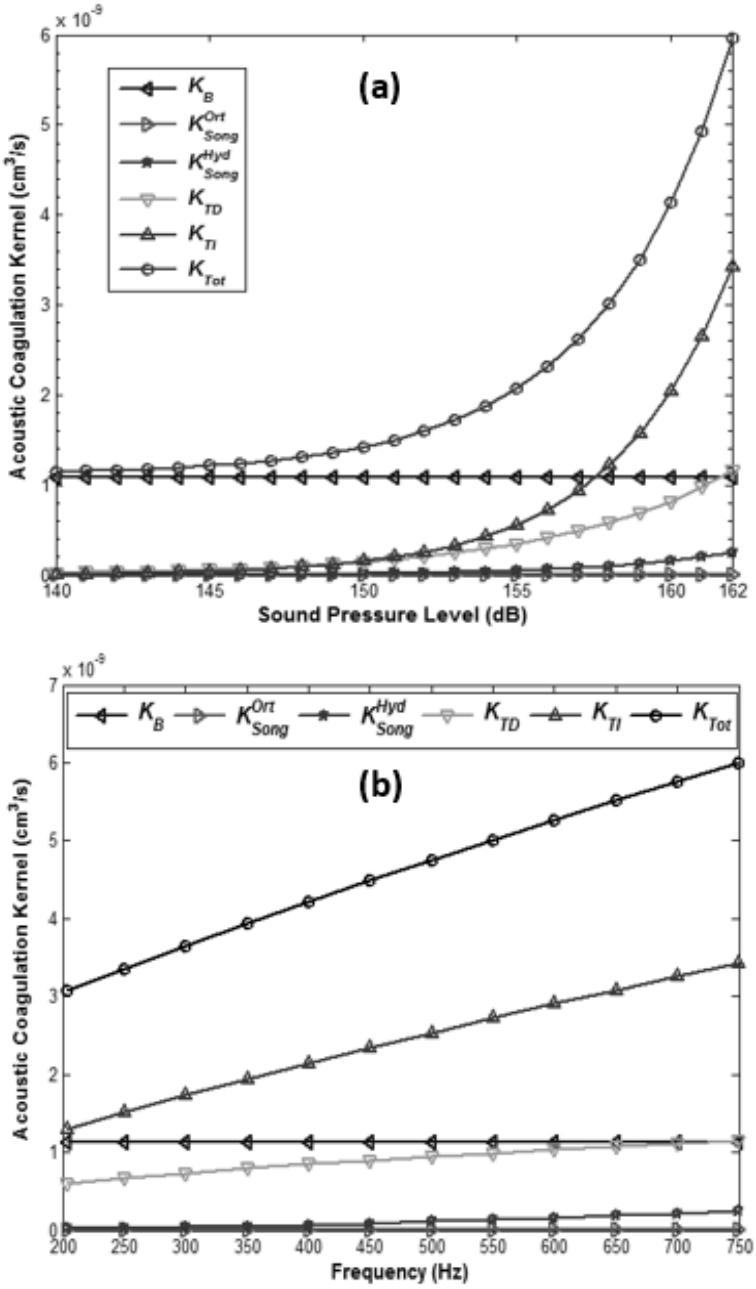

Fig. 3. Evolution of acoustic coagulation kernels (particle-1 (0.3 μm) and particle-2 (0.8 μm)) with respect to the (a) sound pressure level (140–162 dB) at 749 Hz, (b) the frequency (204–749 Hz) at 162 dB.

In order to measure initial concentration of particles, all of the mentioned steps are performed with the exception of using acoustic wave. Due to the effects of Brownian coagulation and sedimentation on the results after desired time, the experiments for measuring initial particle concentration and the particle concentration after using acoustic waves were done in similar time to clarify the net effect of acoustic coagulation and precipitation. It is worth noting that before each experiment there was a separate experiment (by considering similar time) for measuring initial concentration of particles to check the reliability of results. Finally, the averages of the results are reported here.

All experiments were performed in 10 min with similar initial concentration under ambient condition. In this research work, the impact of main parameters including frequency and SPL on the agglomeration and precipitation of particles are investigated.

RESULTS AND DISCUSSION

Particle Precipitation

According to the 16 runs mentioned in the previous section, we investigated the evolution of PSD under the effect of acoustic field. The obtained results are shown in Figs. 6(a)–6(d). The exposure time for these experiments was 10 minutes (t = 10 min).

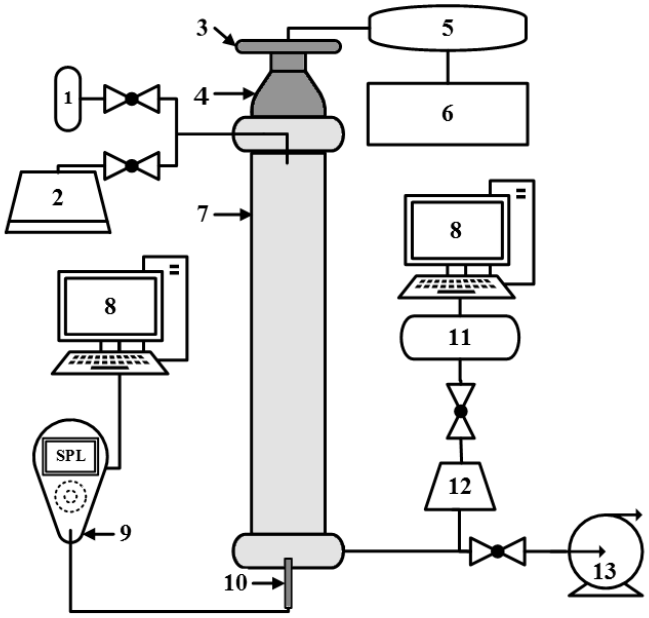

1. Dilution System (Filter-HEPA) **2. Aerosol Generator**
3. Loadspeaker **4. Horn**
5. Power Amplifier **6. Signal Generator**
7. Agglomeration – Precipitation Chamber **8. Computer**
9. Acoustic level recorder **10. Microphone**
11. Particle counter **12. Diluter**
13. Vacuum Pump

Fig 4. A schematic view of Experimental Setup.

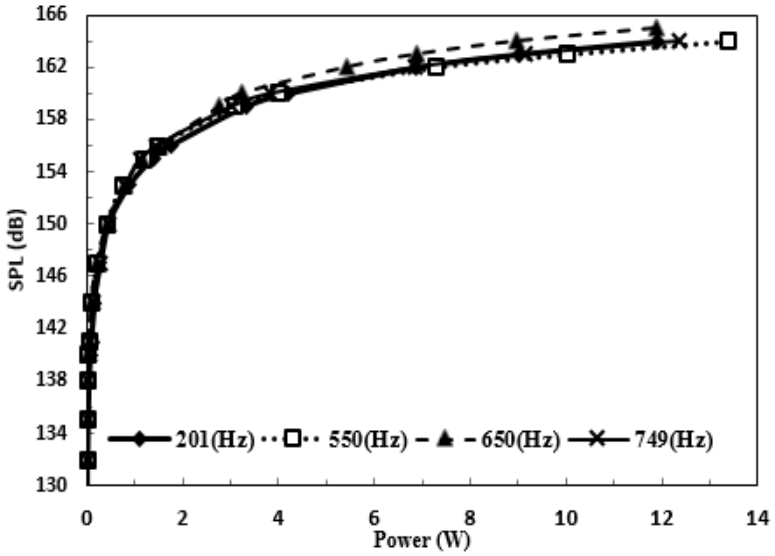

Fig. 5. SPL against Power in different frequencies.

As can be seen in Fig. 6(a), using sound waves with an intensity of 140 dB for 10 minutes caused small changes in the concentration of particles in the range of (0.26–0.45 μm) and even the results are similar by increasing the frequency.

According to Fig. 6(b), in comparison with Fig. 6(a), by using 150 dB sound intensity, no significant difference is seen in the particle size distributions, which indicates that the particles are less prone to coagulation in this sound intensity. However, there is a decrease in the concentration of particles in the range of (0.26–0.45 μm). On the other hand, an increase in concentration of particles in the range of (0.45–2.0 μm) is visible.

In Fig. 6(c), using sound waves with an intensity of 155 dB, as well as reducing the concentration of particles in the range of (0.26–0.45 μm) is a top priority. Furthermore, the concentration of particles larger than (0.45 μm) slightly

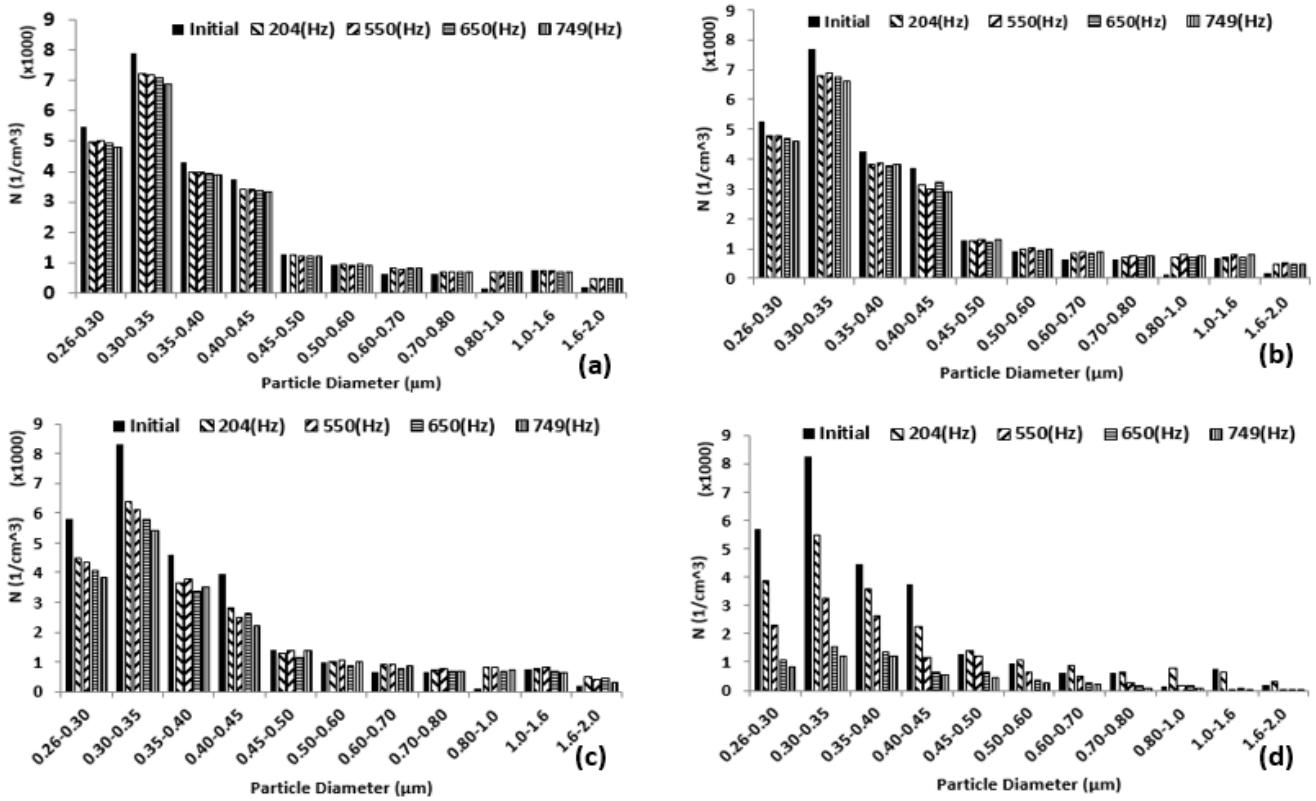

Fig. 6. PSD evolution at different frequencies of acoustic radiation and after 10 min at (a) 140 dB, (b) 150 dB, (c) 155 dB and (d) 162 dB.

changes, representing that the particles coagulation together with formation of larger particles is in the range of (0.45–2µm). In addition, this sound intensity implies that when frequency increases, the particle coagulation improves.

In Fig. 6(d) in comparison with Figs. 6(a), 6(b) and 6(c), changes in PSD pursue another avenue. Such that, at the intensity of 162 dB, the particle concentration decreases nearly at all particle sizes. This suggests that, in addition to the decrease, which occurs due to the coagulation of the fine particles to each other, the particles precipitate to the wall column. At 162 dB, due to the high sound intensity, the probability of creation the powerful turbulence in the milieu increases, which strongly supports the hypothesis of precipitation and coagulation of particles under the eddies impact.

According to Figs. 6(a)–6(d), two points can be noted. Firstly, particle number concentration in the range of (0.26–0.45 µm) decreases by increasing the sound pressure level, which is impressive at the 162 dB. Secondly, the number concentration of particles decreases with increasing frequency, particularly at 162 dB. The different behavior is observed at the frequency of 204 Hz, which indicates the low performance of acoustic coagulation and precipitation at this frequency. As previously mentioned, the phenomenon of turbulence can be an essential factor in changing the behavior of system and improving performance of acoustic precipitation.

It is noteworthy that in the intensity of 140–150 dB, the shape of PSD is closely similar for all frequencies. However, with the intensities of 155 and 162 dBs, the positive effect of improving frequency on the diminishing of particle number concentration is more visible, especially at 162 dB. This phenomenon was also seen in the studies of Sadighzadeh (1990) and Malherbe (1988) denoting that there is a threshold for sound intensity. Moreover, the mechanisms that cause coagulation and precipitation of particles are more dependent on frequency in 162 dB. In section *Acoustic coagulation and precipitation efficiency*, the existence of a threshold for sound intensity will be discussed from another aspect.

Particles Coagulation

To better understand the effects of parameters on the acoustic coagulation of submicron particles, changes of (N_i/N_{i0}) are shown in Figs. 7(a)–7(d). N_{i0} is related to the measured number concentration of each category of particle diameter without using acoustic waves after 10 min. N_i is related to the measured number concentration of each category of particle diameter after using acoustic waves in chamber for 10 min.

By studying the changes in Figs. 7(a)–7(d), which are shown on logarithmic scale in axis (N_i/N_{i0}), acoustic particle coagulation can be observed quite clearly. If $(N_i/N_{i0}) < 1$, the number concentration of particles in category of (i) diameter have been reduced in the presence of acoustic waves. If $(N_i/N_{i0}) > 1$, the number concentration of particles in category (i) have been increased indicating that coagulation of particle in that range of diameter.

As mentioned about Fig. 6(a), the amount of difference

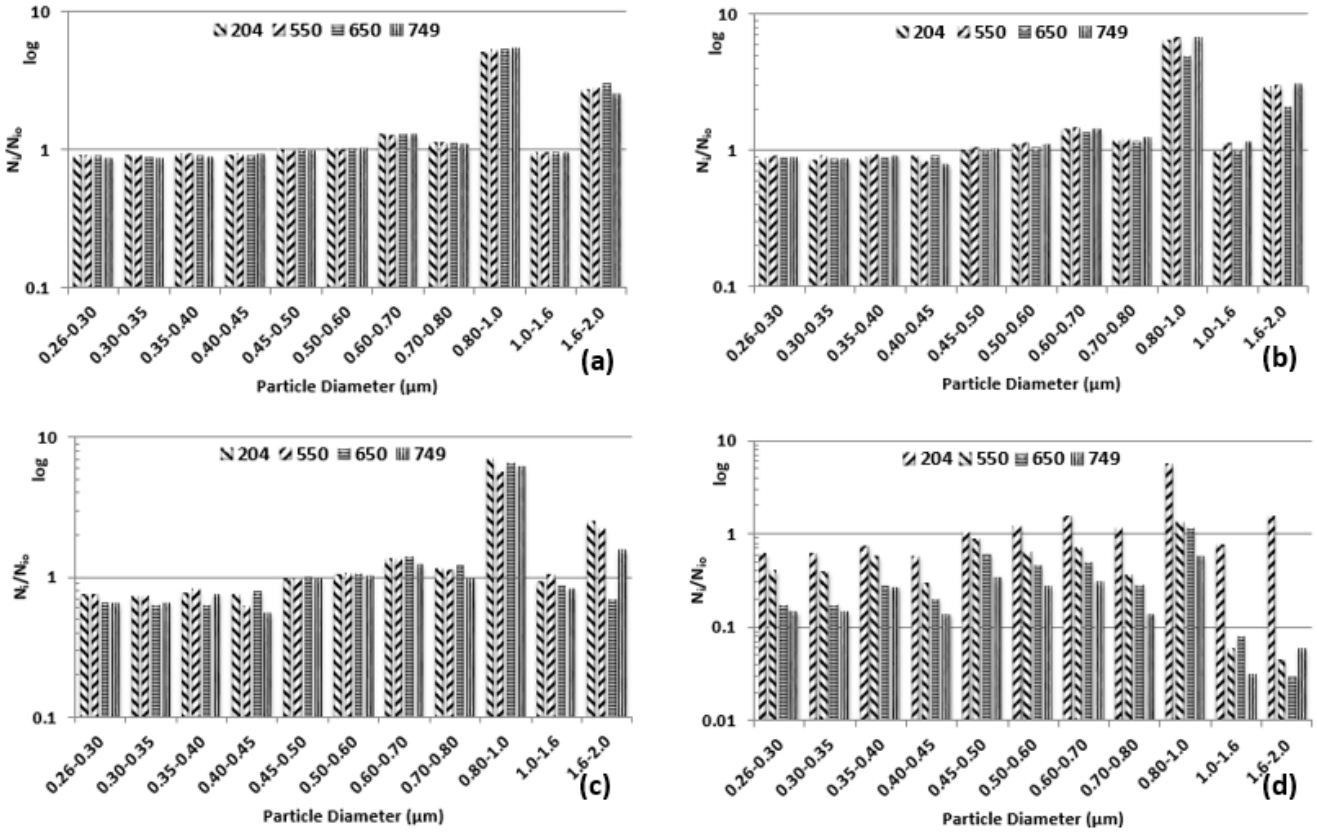

Fig. 7. Evolution of (N_i/N_{i0}) against Frequency (Hz) and after 10 min at (a) 140 dB, (b) 150 dB, (c) 155 dB and (d) 162 dB.

in the concentration ratio of particles in the range of (0.26–0.45 μm) is negligible with the sound intensity of 140 dB. On the other hand, in the range of (0.45–2 μm) the concentration ratio increases. These variations are virtually because of coagulation of fine particles and formation of larger ones. In addition, no significant difference in the results is detected by increasing frequency at this sound intensity.

Similar to Fig. 7(a), in Fig. 7(b) there is a reduction in the concentration ratio of particles in the range of (0.26–0.45 μm) and an increase in the range of (0.45–2 μm); in other words, the effect of increasing frequency on the results is minimal.

According to Fig. 7(c), if acoustic waves were used in the intensity of 155 dB, the amount of concentration ratio reduction in the range of (0.26–45 μm) would be more than the prior intensities. However, beside this reduction, no more improvement is seen in the concentration ratio of particles in the range of (0.45–2 μm), which indicates that in addition to the coagulation mechanism for changing of particle concentration, another mechanism occurs at this sound intensity which is called *acoustic precipitation*. Likewise, at the frequency of 749 Hz, the results show the best reduction performance in the range of (0.26–0.45 μm).

As obviously seen in Fig. 7(d), there are significant reductions in concentration ratio of all particle sizes. In addition, positive effects of frequency on the particle reduction performance can be seen more. It can be suggested that at this sound intensity, the predominant mechanism for reducing particle concentration is acoustic precipitation on the wall column.

Generally, two different behaviors can be observed in these figures. Firstly, in Fig. 7(a), which relates to 140 dB sound intensity, a reduction in the ratio of (N_i/N_{i0}) for particles (0.26–0.45 μm) is illustrated. On the other hand, for particles with diameter of more than 0.45 μm, the ratio of (N_i/N_{i0}) is more than or near one which suggests the coagulation of finer particles. Increasing intensity from 140 to 150 dB causes the intensification of this subject (Figs. 7(a) and 7(b)). However, conditions vary in the intensities of 155 and 162 dBs; apart from the 204 Hz frequency, especially in 162 dB in all particle sizes a considerable reduction in the ratio can be discerned (Figs. 7(c) and 7(d)). This issue can explain that due to the induced turbulence, intensity acoustic precipitation at this sound becomes a predominant phenomenon compared with the particle coagulation mechanism and cause a reduction in the ratio (N_i/N_{i0}), as shown theoretically in Figs. 2 and 3. Secondly, with increasing the frequency from 550 to 749 Hz, the number concentration of particles (N_i) in the range of (0.26–0.45 μm) is reduced with respect to initial concentration (N_{i0}) as the [$(N_i/N_{i0}) << 1$: i = 0.26–0.4]. Instead, the ratio of number concentration of particles in the range of (0.45–1 μm) is not decreased as much as the one for finer particles; it is due to the coagulation of finer particles which generates larger ones. It is worth noting that the initial number concentration of particle in the range of (0.4–1 μm) is infinitesimal (which indicate additional particles in this category is because of the coagulation of finer particles). On the other hand, the percentage of particles in the range of

(1.6–2 μm) is diminished drastically, which strengthens the idea that large particles act as coagulation nuclei. Similar behavior of particles coagulation phenomena is observed in all diagrams. Besides, the particle number concentration decreases considerably when frequency increases, denoting the positive effect of frequency.

Acoustic Coagulation and Precipitation Efficiency

In order to analyze the frequency and SPL effects from another perspective, the acoustic coagulation and precipitation efficiency, which is defined as $\gamma_n = 100 \times (1 - N_{TF}/N_{TI})$, is evaluated. N_{TI} is the total initial particle concentration and N_{TF} is the final total particle concentration in each experimental study. The more the particles concentration reduces, the more acoustic coagulation and precipitation efficiency γ_n is achieved. Fig. 8(a) shows the variation of acoustic coagulation and precipitation efficiency with respect to the SPL in different frequencies. As can be observed, up to about 150 dB there is not much change in the efficiency of this operation. After that, in the 155 dB a significant growth is clearly observed which implies the importance of the SPL threshold in the experiment.

In addition to the effect of frequency on the coagulation of particles, in Fig. 8(a) the increasing trend of acoustic coagulation and precipitation efficiency with respect to (SPL) and different frequencies are shown. However, the curvature of variation at 204 Hz has a gradual slope. Therefore, it suggests that the coagulation mechanisms do not change at this frequency as much as other frequencies, that the efficiency ultimately reaches about 40%. The effect of frequency at 162 dB (SPL) is more significant than others are (γ_n = 83%).

According to Fig. 8(a), the performance increases with high frequencies, however, these increases do not make a significant difference. Our results (Fig. 8(a)) demonstrate a threshold in the acoustic pressure level 155 dB above

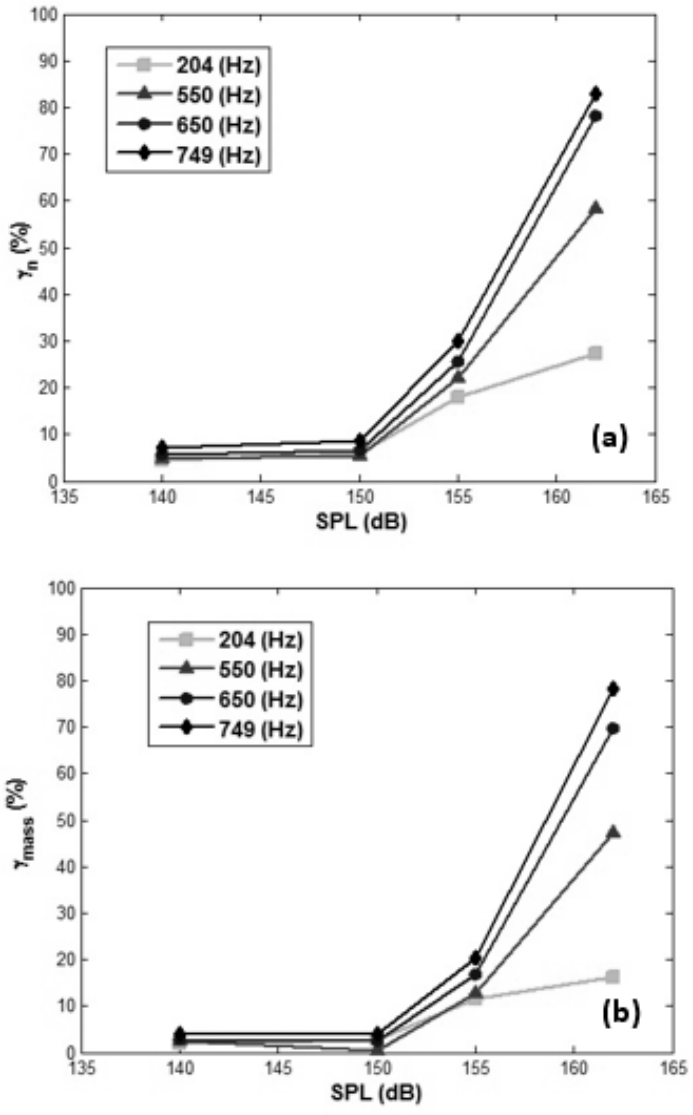

Fig. 8. Variation of (a) acoustic coagulation and precipitation efficiency (γ_n) and (b) acoustic precipitation efficiency (γ_{mass}), against SPL in the different frequencies after 10 min.

which the acoustic coagulation and precipitation efficiency β increases rapidly. This conclusion agrees with the results obtained from the experiments of Malherbe *et al.* (1988) and Sadighzadeh (1990).

As shown in Figs. 3(c) and 3(d), the most important mechanisms at high intensity acoustic wave (≥ 155) are turbulent interactions. Thus, turbulent interactions are responsible for the most of particle coagulations especially at 162 dB.

Moreover, we can study the particle removal from another aspect. Precipitation efficiency could be determined from the particle mass concentration (W_i) instead of using the particle number concentration (N_i), as $\gamma_{mass} = (1 - W_{TF}/W_{TI}) \times 100$. W_i is easily obtained by multiplying N_i by mass of submicron particle i. W_{TI} is the total initial particle mass concentration and W_{TF} is the final total particle mass concentration in each experimental study. Fig. 8(b) shows the variation of acoustic precipitation efficiency γ_{mass} with respect to the SPL in different frequencies. The results of Figs. 8(a) and 8(b) are similar, which represent important particle precipitation along with particle coagulation in the chamber.

Based on the diagram in Fig. 8(b), a novel empirical correlation is evaluated which is defined as follows.

$$\gamma_n(\%) = (0.01143) \times e^{(0.1553 \times SPL - 21.742)} \times \text{Frequency}^{0.8266} \quad (16)$$

where γ(%) is acoustic coagulation and precipitation efficiency percentage.

The 3D graph shown in Fig. 9(a) compares the experimental data with the predicted values by our empirical model which has a high accuracy ($R^2 = 0.975$). The empirical correlation relates acoustic coagulation and precipitation efficiency to SPL and frequency that are two important parameters in this system. Effect of SPL in this correlation

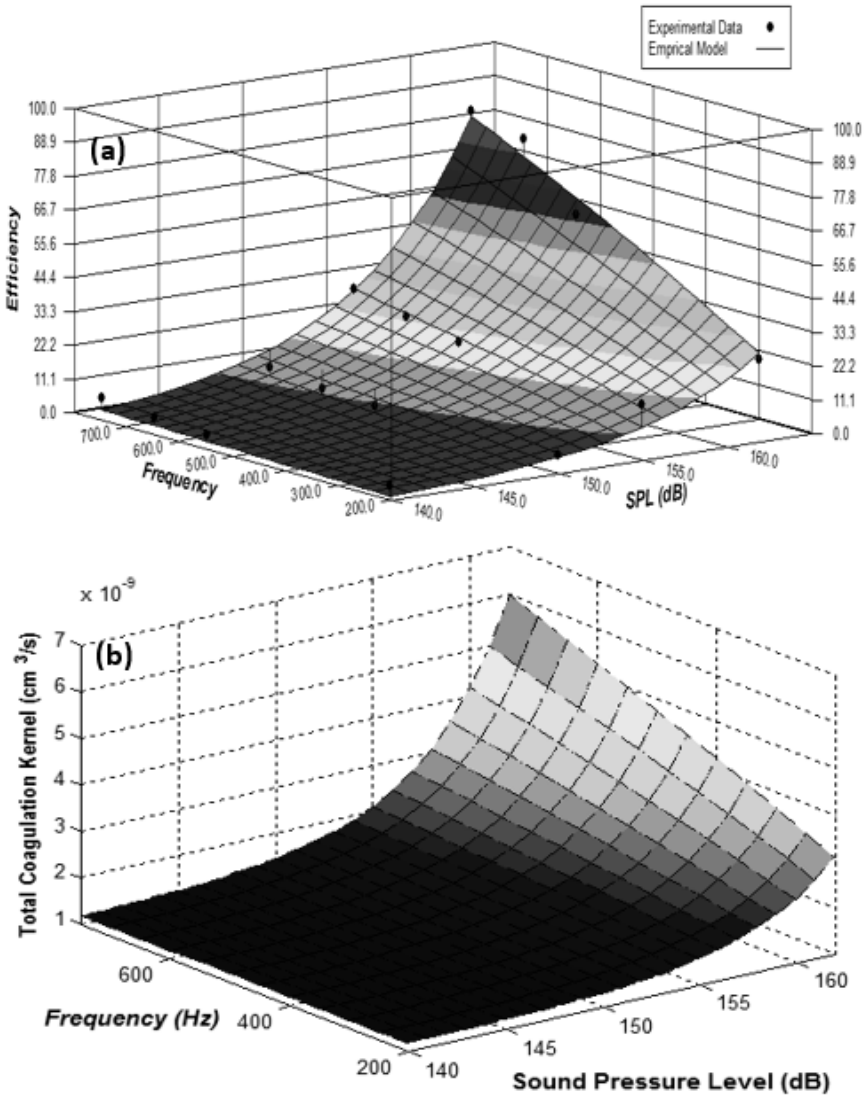

Fig. 9. (a) Comparison of experimental data and predicted value by the empirical model, (b) Evolution of acoustic coagulation kernels (particle-1 (0.3 μm) and particle-2 (0.8 μm)) with respect to the frequency (204–749 Hz) and sound pressure level (140–162 dB).

is more than frequency based on exponential term. Development of K_{Tot} (Eq. (14)) with respect to the both SPL (140–162 dB) and frequency (204–749 Hz) in a 3-dimentional figure is shown in Fig. 9(b). Obviously, both SPL and frequency have positive effect on total acoustic coagulation kernel in the range of specified variables. Since K^{Tot} is used in dynamic evolution of particles equation (Eq. (1)), it is expected that similar progress of particle number concentration occurs in corresponding range of variables. The similarity in trend of empirical correlation Fig. 9(a) and theoretically study Fig. 9(b) approves the hypothesis that at high intensity acoustic waves the dominant mechanism is turbulent coagulation. Since that, the considerable growth in K_{Tot} arises after SPL 155 dB, for which the most important reason is the rapid improvements of turbulent kernels (K^{TI} and K^{TD}).

CONCLUSIONS

In this paper, the effect of acoustic waves on aerosol precipitation and agglomeration was investigated. The influences of two important parameters, including frequency and SPL, were also studied. The main results are as follows: (1) Theoretical study showed that Brownian coagulation is the most important mechanism for coagulation of submicron particles. Furthermore, turbulent interaction is the dominant mechanism for coagulation between a submicron particle and particles larger than one-micron size. (2) Based on theoretical study of acoustic coagulation kernels both frequency and SPL have positive effects on the value of coagulation kernels. In addition, Brownian coagulation is the dominant mechanism in the range of (140–150 dB). However, when sound pressure level rises more than 155 dB, total coagulation kernel increase sharply which is mainly due to the enhancement of turbulence coagulation kernels. (3) By increasing frequency from 204 Hz to 749 Hz, the PSD peak is shifted towards larger particles, indicating the positive effect of the frequency parameter on the acoustic coagulation. (4) The effect of frequency at 162 dB (SPL) is more significant than others, reaching γ_n = 83% at the frequency of 749 Hz, which implies the presence of strong interactions (such as turbulence interactions) at high intensity acoustic waves (≥ 155 dB). (5) A novel empirical equation is developed which relates coagulation and precipitation efficiency to the frequency and SPL. This model shows a good consistency with the experimental data. In addition, similar variation of coagulation and precipitation efficiency and total coagulation kernel is in good agreement with theoretical and experimental results. (6) The results of this study (experimentally and theoretically) prove a threshold in SPL 155 dB above which the acoustic precipitation and coagulation efficiency increase rapidly, implying the importance of turbulence coagulation interactions at high intensity acoustic waves.

REFERENCES

Brandt, O. and Hiedemann, E. (1936). The aggregation of suspended particles in gases by sonic and supersonic waves. *Trans. Faraday Soc.* 32: 1101–1110.

Cheng, M.T., Lee, P.S., Berner, A. and Shaw, D.T. (1983). Orthokinetic agglomeration in an intense acoustic field. *J. Colloid Interface Sci.* 91: 176–187.

Chou, K.H., Lee, P.S. and Shaw, D.T. (1981). Aerosol agglomeration in high-intensity acoustic fields. *J. Colloid Interface Sci.* 83: 335–353.

Crowe, C.T. (2005). *Multiphase Flow Handbook*. Taylor and Francis.

Danilov, S.D. and Mironov, M.A. (1984). Radiation pressure force acting on a small particle in a sound field. *Sov. Phys. Acoust.* 30: 280–283.

Dong, S., Lipkens, B. and Cameron, T.M. (2006). The effects of orthokinetic collision, acoustic wake, and gravity on acoustic agglomeration of polydisperse aerosols. *J. Aerosol Sci.* 37: 540–553.

Ezekoye, O.A. and Wibowo, Y.W. (1999). Simulation of acoustic agglomeration processes using a sectional algorithm. *J. Aerosol Sci.* 30: 1117–1138.

Gallego-Juárez, J.A., Riera-Franco De Sarabia, E., RodrÍguez-Corral, G., Hoffmann, T.L., Gálvez-Moraleda, J.C., RodrÍguez-Maroto, J.J., Gómez-Moreno, F.J., Bahillo-Ruiz, A., MartÍn-Espigares, M. and Acha, M. (1999). Application of acoustic agglomeration to reduce fine particle emissions from coal combustion plants. *Environ. Sci. Technol.* 33: 3843–3849.

Guo, Q., Yang, Z. and Zhang, J. (2012). Influence of a combined external field on the agglomeration of inhalable particles from a coal combustion plant. *Powder Technol.* 227: 67–73.

Lee, P.S., Cheng, M.T. and Shaw, D.T. (1981). The influence of hydrodynamic turbulence on acoustic turbulent agglomeration. *Aerosol Sci. Technol.* 1: 47–58.

Levich, V.G. (1962). *Physicochemical Hydrodynamics*. Prentice-Hall, Englewood Cliffs, N.J.

Liu, J., Zhang, G., Zhou, J., Wang, J., Zhao, W. and Cen, K. (2009). Experimental study of acoustic agglomeration of coal-fired fly ash particles at low frequencies. *Powder Technol.* 193: 20–25.

Malherbe, C., Boulaud, D., Boutier, A. and Lefevre, J. (1988). Turbulence induced by an acoustic field application to acoustic agglomeration. *Aerosol Sci. Technol.* 9: 93–103.

Martin, K.M. and Ezekoye, O.A. (1997). Acoustic filtration and sedimentation of soot particles. *Exp. Fluids* 23: 483–488.

Mednikov, E.P. (1965). *Acoustic Coagulation and Precipitation of Aerosols*. Consultants Bureau, New York.

Patterson, H.S. and Cawood, W. (1931). Phenomena in a sounding tube. *Nature* 127: 667.

Sadighzadeh, A. (1990). *Etude De L'efficacité De Capitation Des Aerosol Par Un Lit Granulaire En L'absence Et En Presence D'ondes Acoustiques*, Paris, France.

Saffman, P.G. and Turner, J.S. (1956). On the collision of drops in turbulent clouds. *J. Fluid Mech.* 1: 16–30.

Shaw, D.T. and Tu, K.W. (1979). Acoustic particle agglomeration due to hydrodynamic interaction between monodisperse aerosols. *J. Aerosol Sci.* 10: 317–328.

Sheng, C. and Shen, X. (2006). Modelling of acoustic

agglomeration processes using the direct simulation Monte Carlo methodd. *J. Aerosol Sci.* 37: 16–36.

Smoluchowski, M. (1916). Drei vorträge über diffusion, brownsche molekularbewegung und koagulation von kolloidteilchen. *Physik. Z.* 17: 557–599.

Somers, J., Magill, J., Richter, K., Fourcaudot, S., Lajarge, P. and Barraux, P. (1991). Acoustic agglomeration of liquid and solid aerosols: A comparison of a glycol fog and titanium dioxide. *J. Aerosol Sci.* 22: S109–S112.

Song, L. (1990). *Modeling of Acoustic Agglomeration of Fine Aerosol Particles*, the Pennsylvania State University.

Song, L., Koopmann, G.H. and Hoffmann, T.L. (1994). An improved theoretical model of acoustic agglomeration. *J. Vib. Acoust.* 116: 208–214.

Tavossi, H. (1986). Effects of an acoustic wave on the aerosol collection efficiency of a packed-bed of spheres. *Langmuir* 2: 757–760.

Temkin, S. (1994). Gasdynamic agglomeration of aerosols. I. Acoustic waves. *Phys. Fluids* 6: 2294–2303.

Vincent, J.H. (1995). *Aerosol Science for Industrial Hygienists*. Elsevier science.

Wang, J., Liu, J., Zhang, G., Zhou, J. and Cen, K. (2011). Orthogonal design process optimization and single factor analysis for bimodal acoustic agglomeration. *Powder Technol.* 210: 315–322.

Wood, R.W. and Loomis, A.L. (1927). XXXVIII. The physical and biological effects of high-frequency sound-waves of great intensity. *Philos. Mag.* 4: 417–436.

Received for review, December 27, 2015
Revised, April 6, 2016
Accepted, March 2, 2016